Supplemental Figures

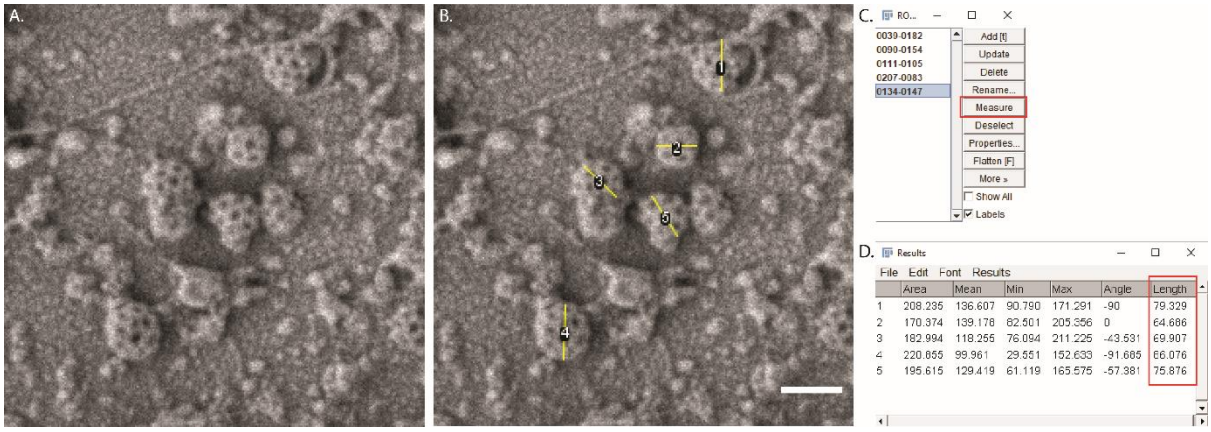

Figure S1 – Measuring the size of CCVs in replica SEM images. (Related to Figure 2).

A) Example CCSs captured by SEM of *Arabidopsis* protoplast metal replicas. B) Line ROIs draw over the diameter of each clearly identify CCS (yellow lines). Scale bar = 100 nm. C) Fiji ROI manager, the red rectangle highlights the measure button used to determine the length of all the ROIs. D) The results of the ROI measurements, the red rectangle highlights the length column of the ROIs.

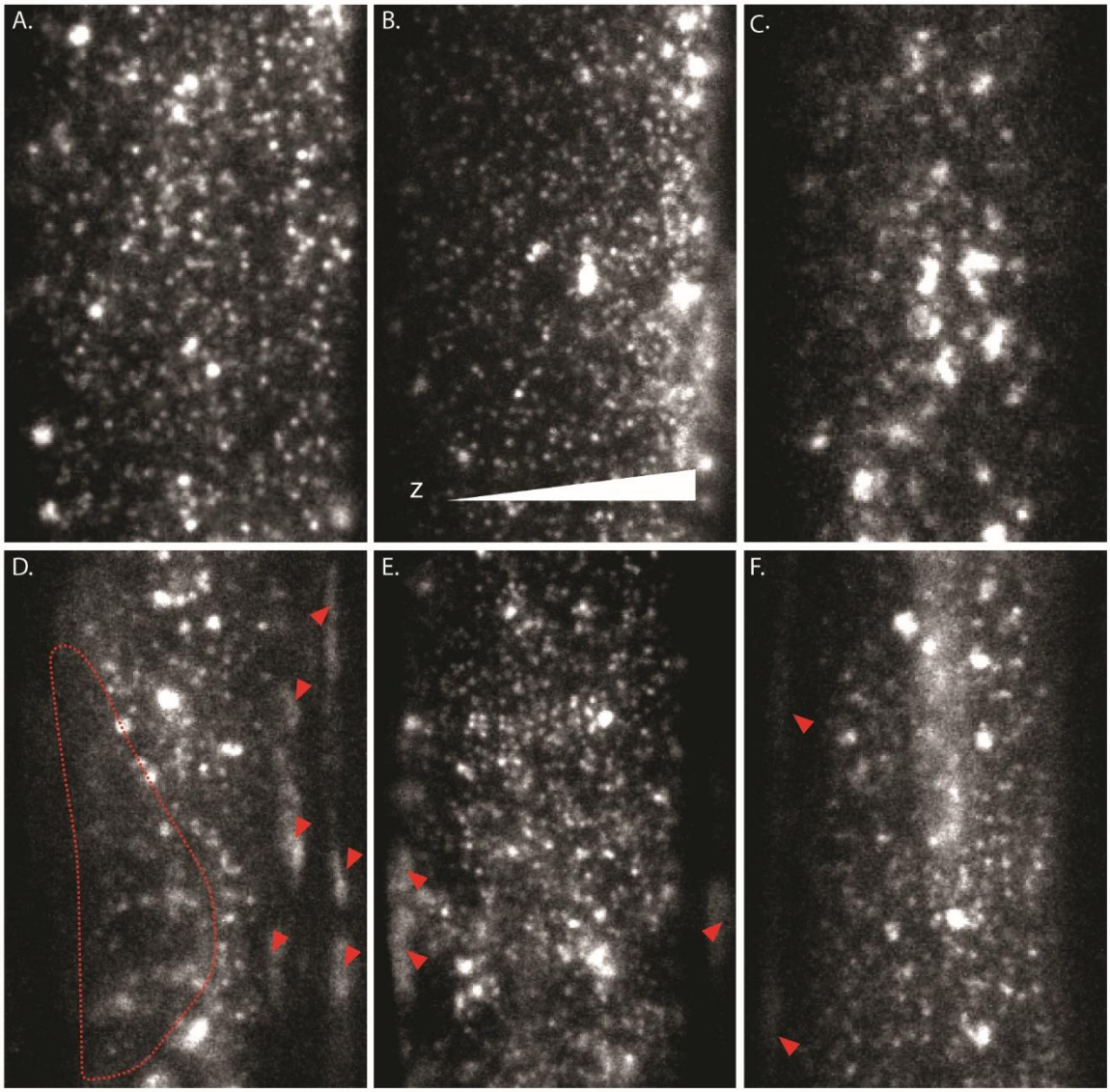

Figure S2 – Comparison of quality of TIRF-M images. (Related to Figures 3, 4 and 5).

Representative TIRF-M image of the epidermal root cells expressing CLC2-GFP. A) shows a good example where the image has a uniform field of illumination across the whole image, and there is an absence of static auto fluorescent signals. Poor examples of TIRF-M images; B) shows image where the TIRF angle is not correctly set, and HILO/VAEM is being used. It is evident based on the non-uniformity of penetration depth of the illumination (white triangle indicates the increase in z penetration), C) shows an out of focus image, D) shows a cell without a flat contact on the coverslip (red dashed line depicts out of contact areas), additionally red arrows note static autofluorescence signals in the field of view, E) shows an image with static autofluorescence signals in the field of view (red arrows), F) shows and image where there is interference of the TIRF-M illumination producing a uniform image of the PM (red-dashed line) and F). Scale bar = 5 µm.

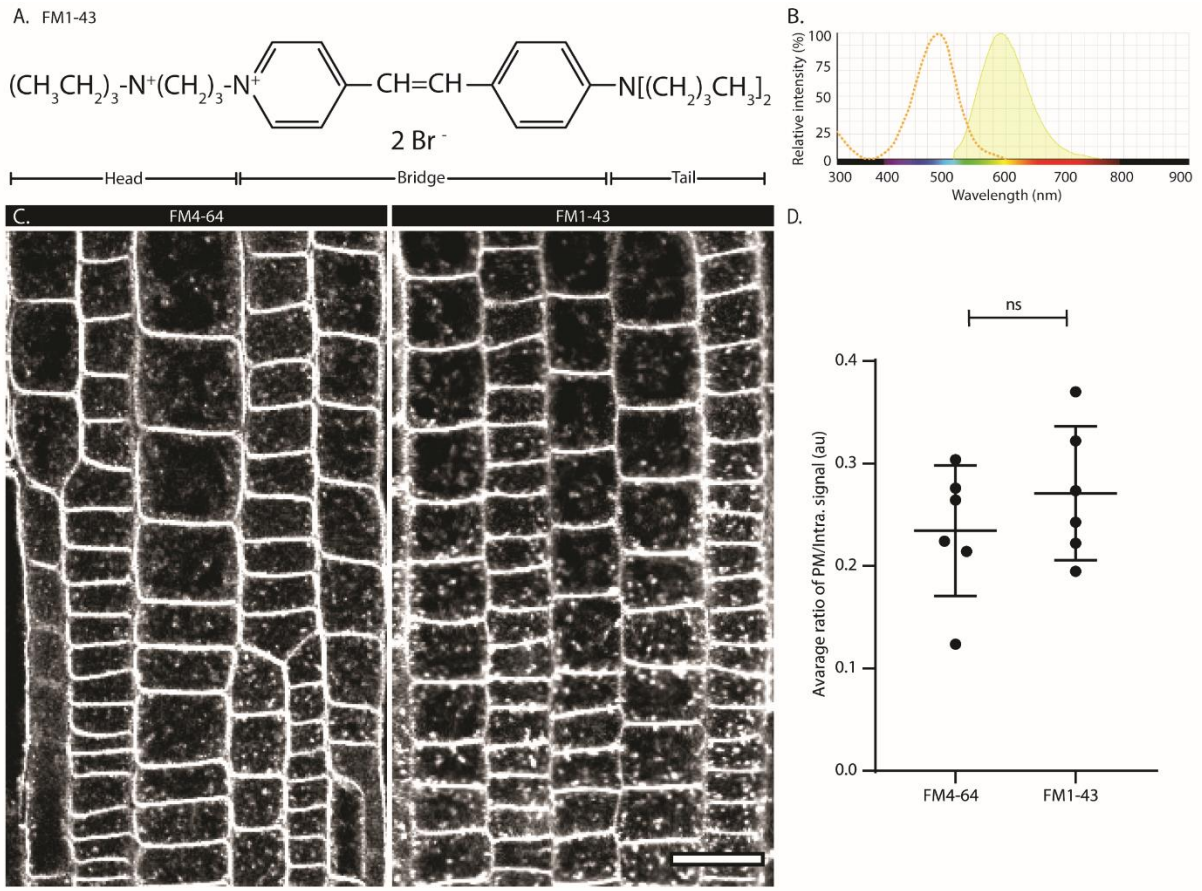

Figure S3 – Comparison of the membrane internalization using FM4-64 and FM1-43. (Related to Figure 6).

A) Chemical structure of FM1-43. B) The fluorescent spectra of FM1-43 (adapted from ThermoFisher bioscience Fluorescence SpectraViewer). C) Representative confocal images of epidermal root cells incubated with FM4-64 and FM1-43. Scale bar = 20 µm. D) Quantification of FM uptake as determined by the ratio of PM and intra-cellular signal. Plots are mean +/- SEM. N, FM4-64 = 6 individual seedlings, 231 cells; FM1-43 = 6 individual seedlings, 139 cells. T-test, *p*-value = 0.3501.

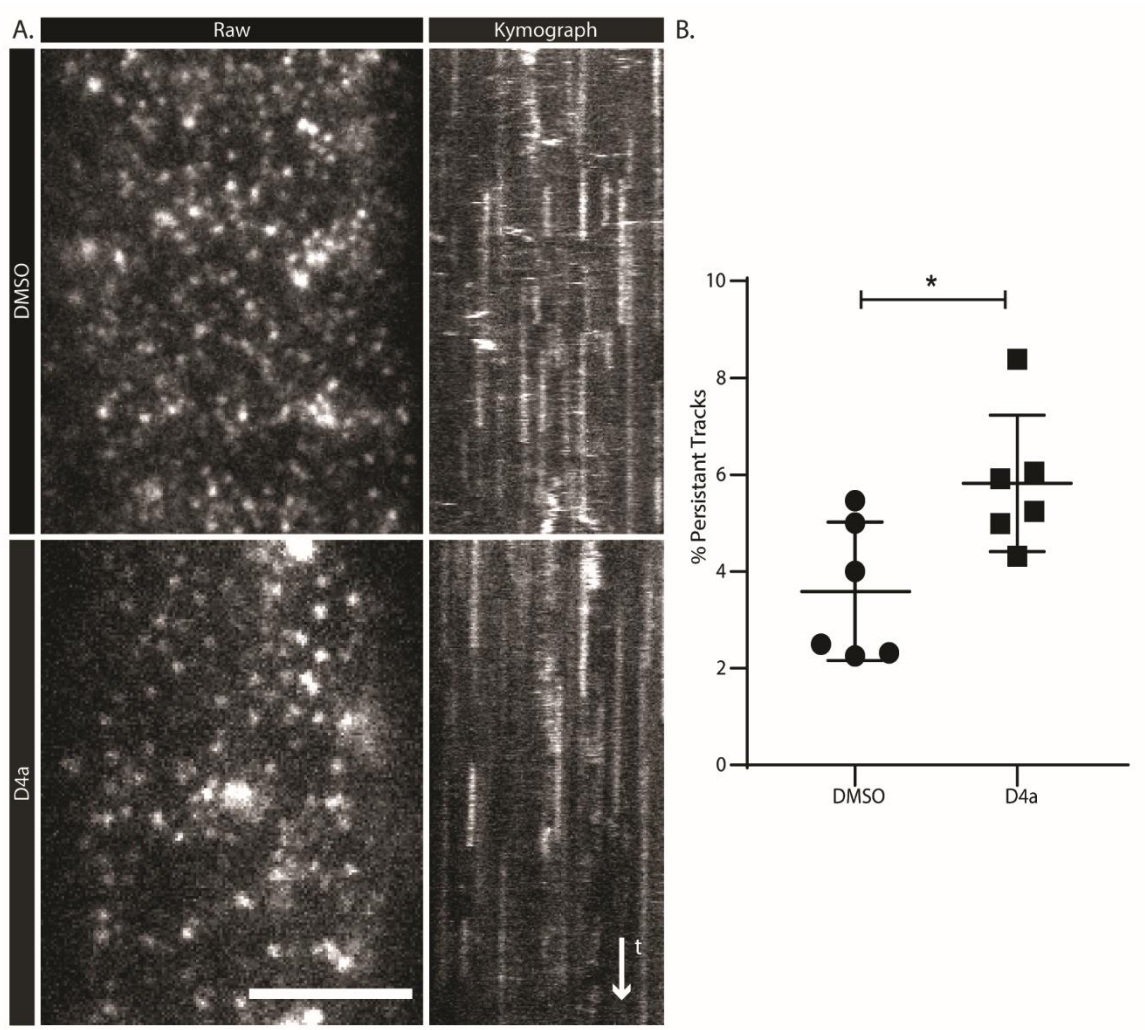

Figure S4 – Effect of Dyngo 4a on CLC-GFP Dynamics.

A) Example of TIRF-M images from the root epidermal cells expressing CLC2-GFP; comparison of mock (DMSO) (upper row) and treatment (Dyngo 4a (D4a), 30µM, 15 min) (lower row). Representative kymographs show the effect of treatment on the PM dynamics of CLC2-GFP. Scale bar = 5 µm. B) Quantification results from combined data of persistent tracks. Plots are mean +/- SEM. N, DMSO = 6 cells from independent roots, 4491 tracks; Dyngo 4a = 6 cells from independent roots, 4700 tracks. T-test, p-value = 0.0217.

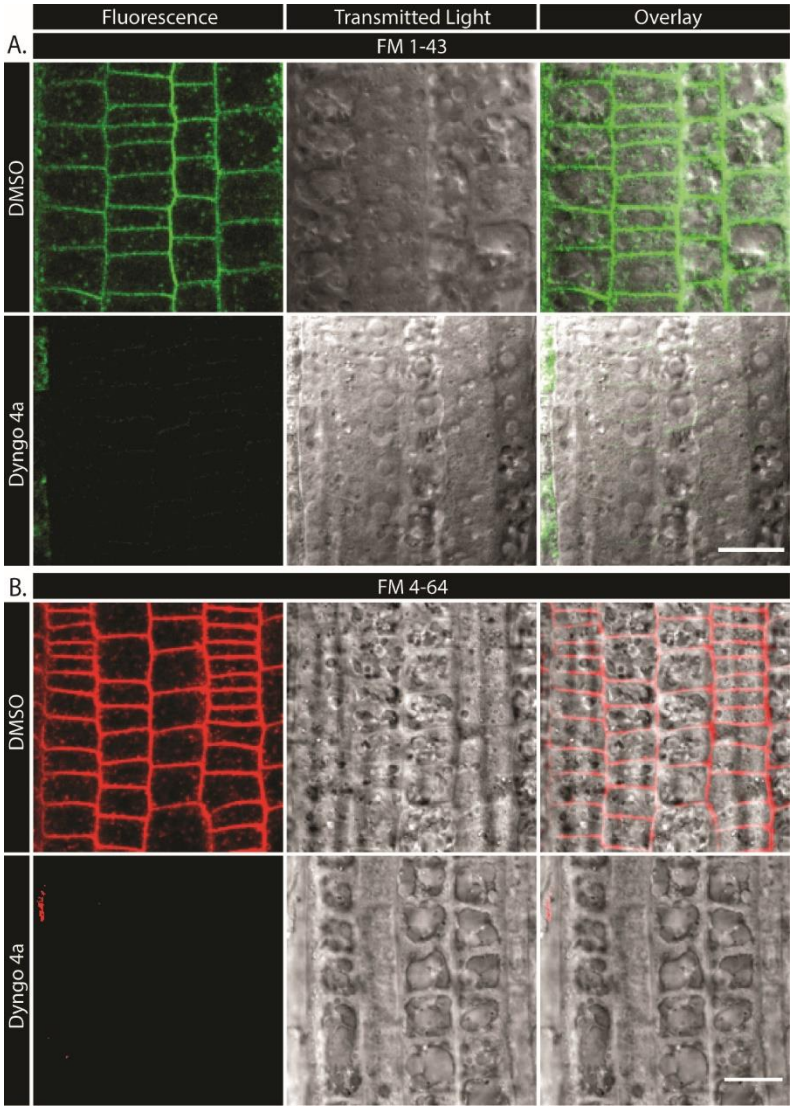

Figure S5 –Dyngo 4a absorbs FM1-43 and FM 4-64 emission. (Related to Figure 6). Representative confocal images of the epidermal root cells, using the same microscope settings, incubated in control (DMSO) or Dyngo 4a (15 mins 30 µM) conditions in the presence of A) FM1-43 or B) FM4-64 membrane dyes. Scale bars = 20 µm.

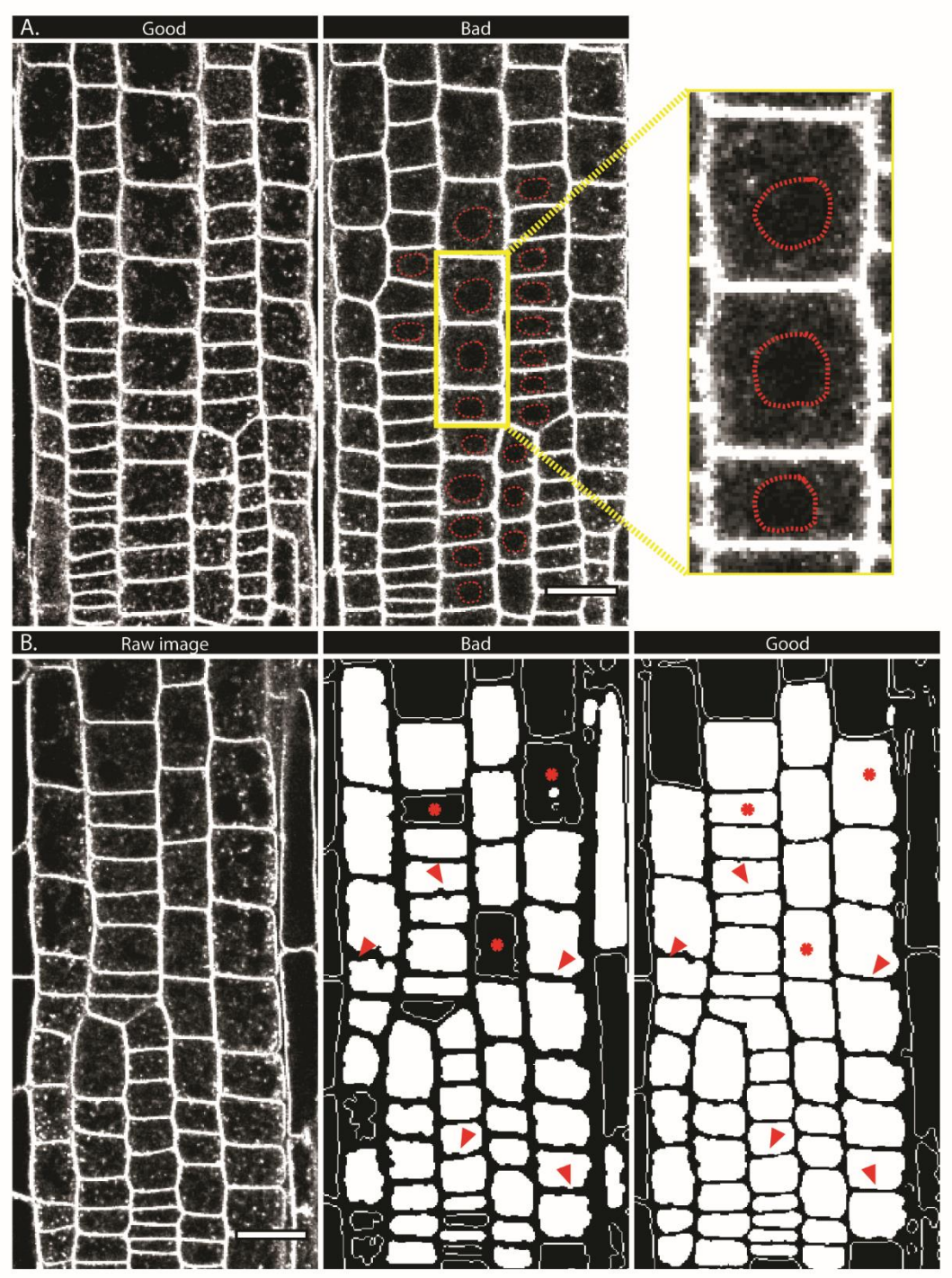

Figure S6 – Comparison of FM cell selection and segmentation. (Related to Figure 6).
A) Examples of poor z plane selection of FM images for analysis. A good example is shown on the left. The bad example (right) has dark black holes in the middles of the cell (red-dashed line outlines the vacuole, image in the middle). The yellow rectangle notes the zoomed in region of the example. B) Representative confocal image of the epidermal root cells incubated with FM4-64 and segmented images with a different threshold. If the threshold for the segmentation of the raw image (on the left) is set incorrectly, the edges of the cells have a lot of prominences (red arrows, middle image). The correct threshold will approximate the outlines to the actual shape of the cells (red arrows, right image). It is important to select only cells which are completely separated and do not interact with the outlines of neighboring cells. Scale bars = 20 µm.

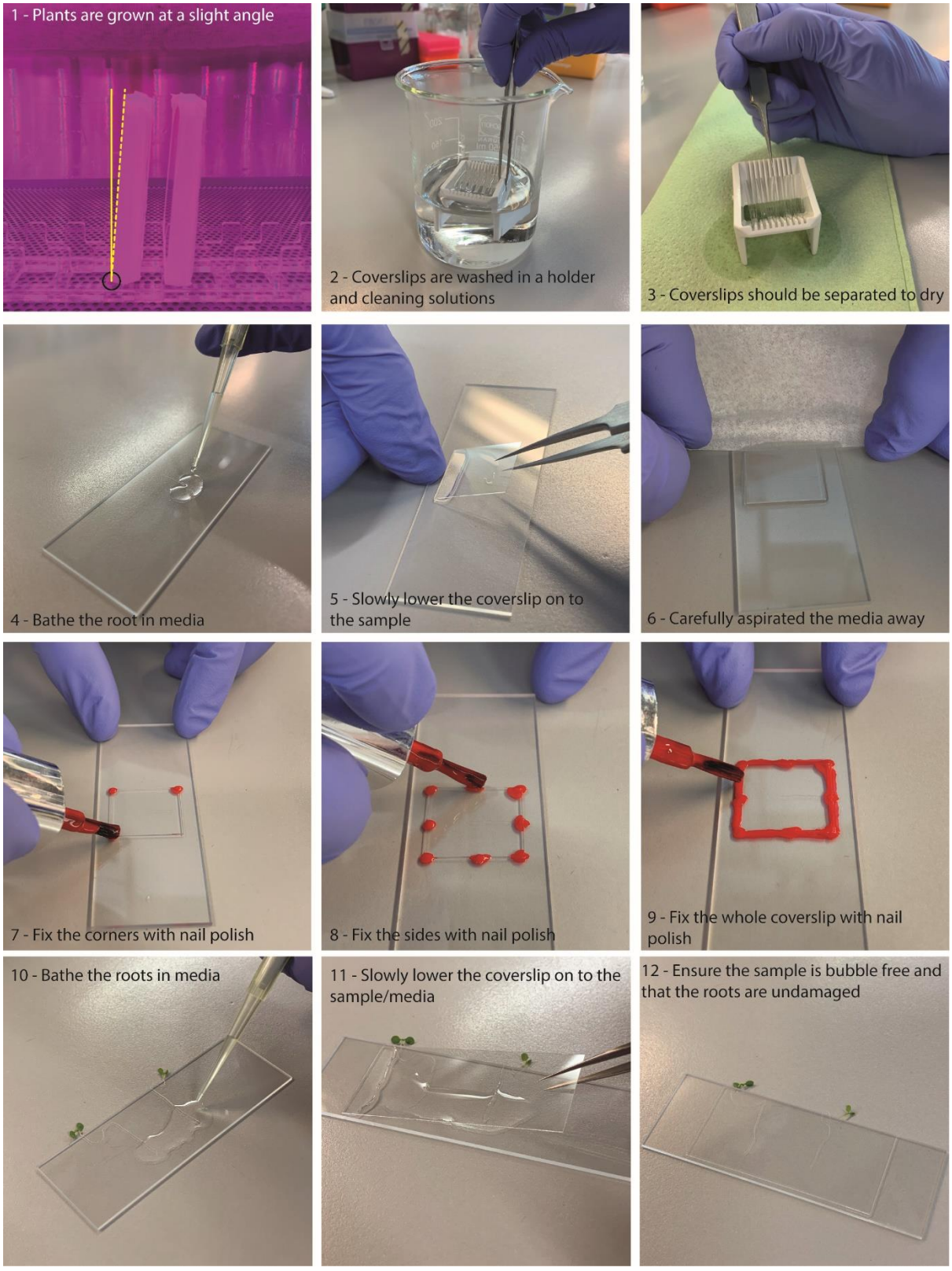

Figure S7

(1-9) Photos of TIRF-M sample preparation. (10-12) photos of FM sample preparation

Supplemental Tables

	EM		TIRF-M	Confocal	
	Resin Sections	**Metal Replica**		**Spinning Disk**	**CLSM**
Effective resolution nm (x,y,z)	4, 4, 40-70	4,4,0*	200, 200, 100	200, 200, ~500	200, 200, 500
Speed	Fixed	Fixed	Fastest	Fast	Slow
Florescence Sensitivity	-	-	High	Low	Low
CME Sample prep ease	Extreme	Hard	Hard	Easy	Easy
Best Application	Ultrastructural analysis		Cell surface imaging		Global uptake assays
Major Pro	Resolution		High signal to noise ratio on cell surface	Can image any tissue type	
Major Con	Fixed		Only cell surface	Low sensitivity for EAPs	

* There is not effective z resolution, as the image is of the surface of the replica.

Table S1 – Comparison of the selected plant CME imaging technologies

Protein	Tag	AGI number	Full Construct	Background/ Ecotype	Functionality	References
AP2A1	GFP	AT5G22770	p35s::AP2A1-GFP	Col-0	-	(Di Rubbo et al., 2013)
AP2A1	YFP	AT5G22770	p35s::AP2A1-YFP	Col-0	-	(Kim et al., 2013)
AP2A1	tagRFP	AT5G22770	pRPS5A::AP2A1-mTagRFP	Col-0	-	(Di Rubbo et al., 2013)
AP2M	GFP	At4g46630	pAP2M-AP2M-GFP	*ap2m*	Complements the significant FM4-64 internalization defect of *ap2m*	(Yamaoka et al., 2013)
AP2M	YFP	At4g46630	pAP2M-AP2M-GFP	*m2-1*/Col-0	Complements the significant FM4-64 internalization defect of *m2-1*	(Bashline et al., 2013)
AP2S	GFP	At1g47830	pAP2S::AP2s-GFP	*ap2s*	Full rescue of the developmental defects of *ap2s*	(Fan et al., 2013)
AP2S	mCherry	At1g47830	pAP2S::AP2s-mCherry	Col-0	-	(Fan et al., 2013)
CHC1	GFP	AT3G11130	pRPS5A::CHC1-GFP	Col-0	-	(Dejonghe et al., 2016, Di Rubbo et al., 2013)
CLC1	GFP	AT2G20760	pCLC1::CLC1-GFP	Col-0	-	(Di Rubbo et al., 2013)
CLC2	mOrange	AT2G40060	pCLC2::CLC2-mOrg	WS and Col-0	-	WS (Konopka et al., 2008); Col-0 (Dejonghe et al., 2016)
CLC2	GFP	AT2G40060	pCLC2::CLC2-GFP	WS and Col-0	-	WS (Konopka et al., 2008); Col-0 (Di Rubbo et al., 2013,

						Fan et al., 2013, Dejonghe et al., 2016)
CLC2	GFP	AT2G40060	pRPS5A::CHC2-GFP	Col-0	-	(Ortiz-Morea et al., 2016)
CLC2	mCherry	AT2G40060	p35s-::CLC2-mCherry	Col-0	-	(Van Damme et al., 2011)
CLC2	tagRFP	AT2G40060	RPS5Ap::CLC2-TagRFP	Col-0	-	(Gadeyne et al., 2014)
CLC3	GFP	AT3G51890	pCLC3::CLC3-GFP	Col-0	-	(Di Rubbo et al., 2013)
Drp1a	mOrange	AT5G42080	pDrp1a::Drp1a-mOrange	*drp1a-2/*WS	Complements the infertility of *drp1a* mutant	(Konopka and Bednarek, 2008)
Drp1a	RFP	AT5G42080	p35s::Drp1a-mRFP1	*drp1a/*Col-0	Rescue of the developmental phenotypes of *drp1a* mutant plants	(Fujimoto et al., 2008, Mravec et al., 2011)
Drp1c	GFP	AT1G14830	pDrp1c::Drp1c-GFP	*drp1c-1/*WS	Rescue of the development of *drp1C-1* pollen	(Konopka et al., 2008)
Drp2a	GFP	AT1G10290	pDrp2a::Drp2a-GFP	Col-0	-	(Huang et al., 2015)
Drp2b	tagRFP	AT1G59610	pDrp2b::Drp2b-tagRFP	Col-0	-	(Huang et al., 2015)
Drp2b	GFP	AT1G59610	p35s::Drp2b-GFP	Col-0	-	(Fujimoto et al., 2008)
TPLATE	GFP	AT3G01780	pTPLATE::TPLATE-GFP	*tplate/*Col-0	Rescue of the homozygous *tplate* mutant	(Gadeyne et al., 2014)
TML	GFP	AT5G57460	pTML::TML-GFP	*tml-1/*Col-0	Rescue of the male transmission failure of both *tml-1/tml-2* mutant allele	(Gadeyne et al., 2014)

TML	YFP	AT5G57460	pTML::TML-YFP	*tml-1*/Col-0	Rescue of the male transmission failure of both *tml-1/tml-2* mutant allele	(Gadeyne et al., 2014)
LOLITA	GFP	AT1G15370	p35s::LOLITA-GFP	Col-0	-	(Gadeyne et al., 2014)
TWD40-2	GFP	AT5G24710	p35s::TWD40-2-GFP	Col-0	-	(Gadeyne et al., 2014)
TWD40-2	GFP	AT5G24710	pTWD40-2::GFP-TWD40-2	*twd40-2-3*/ Col-0	Rescue of the growth defects of *twd40-2-3*	(Bashline et al., 2015)
TASH3	GFP	AT2G07360	p35s::TASH3-GFP	Col-0	-	(Gadeyne et al., 2014)
atEH1	GFP	AT1G20760	p35s::atEH1-GFP	Col-0	-	(Gadeyne et al., 2014)
atEH2	GFP	AT1G21630	p35s::atEH2-GFP	Col-0	-	(Gadeyne et al., 2014)

Table S2 – Examples of key published Fluorescent clathrin and EAP markers lines

Table S2 – Published Fluorescent clathrin and EAP markers lines

Drug	Effect	Mechanism	Notes	Plant Tissue Tested	Ref
Dynasore	Inhibited cargo internalization	Dynamin GTPase inhibitor	Reported off tagged effects on membrane ruffling	*Nicotiana benthamiana*	(Sharfman et al., 2011)
Dyngo 4a	Prolonged CLC2 lifetime, reduced fixable FM uptake, block cargo uptake	Dynamin GTPase inhibitor	Absorbs light 500-700 nm, therefore not suitable for red imaging	Seedlings, *Nicotiana benthamiana*	(Hunter et al., 2019, Zhang et al., 2017) and Figure S5
ES9	Very strong block of FM uptake, prolonged cell surface lifetime of EAPs	Binds CHC	It is a protonophore	Seedlings	(Dejonghe et al., 2016)
ES9-17	Very strong block of FM uptake, prolonged cell surface lifetime of EAPs	Binds CHC	Targets CHC, which is involved in other clathrin mediated processes	Seedlings	(Dejonghe et al., 2019)
IKA	Reduced FM uptake, prolonged cell surface lifetime of EAPs	Unknown	Appears to be specific for CME, however caution should be used as its mechanistic function is unknown	Seedlings, Pollen Tube, BY2 cells	(Bandmann et al., 2012, Elkin et al., 2016, Moscatelli et al., 2007) and Figures 7 and 8
Pitstop-2	Reduced FM uptake	Disrupts clathrin interactions	Not CME specific and did not effect block internalization of cargo	Seedlings	(Dejonghe et al., 2019, Dutta et al., 2012, von Kleist et al., 2011)

Table S3 – Chemical inhibitors of plant CME

Protein	Gene	AGI number	Function in CME	Modification	Phenotype	Tissue	References
Clathrin	*CHC1*	AT3G11130	Formation of clathrin triskelion	pINTAM>>RFP-HUB1	Endocytic defect (inhibition of FM4-64 internalization)	Root, BY-2 cells	(Dhonukshe et al., 2007), (Tahara et al., 2007), (Robert et al., 2010) , (Kitakura et al., 2011)
AP-2	*AP2A1*	AT5G22770	Adaptor complex that interacts with the membrane, clathrin, and CME accessory proteins and cargo	AP2A-RNAi	Endocytic defect (inhibition of FM4-64 internalization in root epidermal cells)	Root	(Di Rubbo et al., 2013)
	AP2A2	AT5G22780					
	AP2M	AT5G46630		AP2MΔC	Endocytic defect (inhibition of FM4-64 internalization in root epidermal cells, defect in formation of BFA bodies)	Root	(Di Rubbo et al., 2013), (Owen and Evans, 1998)
AP180	*AP180*	AT1G05020	Adaptor protein involved in clathrin-mediated endocytosis	At-AP180ΔENTH truncated version	No showed effect *in vitro*	Cell suspension cultures of *A. thaliana*	(Barth and Holstein, 2004)
Dynamins	*DRP1A*	AT5G42080	CCV scission from PM / Putative role in CCV scission	K47A point mutation in GTPase domain	Longer CLC lifetime	Root	(Yoshinari et al., 2016)
	DRP2A	AT1G10290		Inducible Strep-DRP2A-K51E	Endocytic defect (reduced endocytosis in root hairs; bulging of the tip of root hairs,	Root	(Taylor et al., 2011)
	DRP2B	AT1G59610		Inducible Strep-DRP2B-K51E			

					and bursting of root hairs at the very tip) Mutant cannot complement the knock -out phenotype		
	DRP1E	AT3G60190	Potentially involved in CCV scission from PM	P77L point mutation in GTPase domain	gain-of-function phenotype	Root	(Tang et al., 2006)
Auxilin	*AUXILIN-LIKE1*	AT4G12780	Negative regulation of endocytosis	XVE»AUXILIN-LIKE1/2	Block of endocytosis after the initial step by inhibition of recruitment of clathrin	Root	(Adamowski et al., 2018, Ortiz-Morea et al., 2016)
TPLATE complex	*TML*	AT5G57460	TPLATE complex subunit involved in clathrin mediated endocytosis.	Truncated TML TMLΔC	Endocytic defect (inhibition of FM4-64 internalization, defect in formation of BFA bodies, reduction in TPC complex size)	Root	(Gadeyne et al., 2014)
				amiR-TML			
	TPLATE	AT3G01780		*amiR-TPLATE*	Endocytic defect (inhibition of FM4-64 internalization, defect in formation of BFA bodies)		

Table S4 – Published genetic manipulations of plant CME

	FM	Photoconvertible fluorophore (e.g., Dendra)	BFA
Tissue tested	Protoplasts and plants	Plants	Protoplasts and plants
Ease	Application/incubation of dye	Requires cloning and transformation	Application/incubation of compound
Specificity	Not specific for CME, but total PM internalization	Dependent on cargo studied	Dependent on cargo studied
Pros	Rapid and direct measure of PM endocytosis	Specific for a certain cargo	Rapid to establish assay
Cons	Not specific for CME	Takes time to generate material and cargo pathway must be known	Artificial BFA body

Table S5 – Summary of example global uptake methods

Protein	Gene	AGI number	Phenotype	References
Clathrin	*chc1*	AT3G11130	Reduced rates of endocytosis and defects clathrin mediated exocytosis	(Alonso et al., 2003), (Kitakura et al., 2011), (Larson et al., 2017)
	chc2	AT3G08530	Reduced rates of endocytosis and defects clathrin mediated exocytosis	
	clc1	AT2G40060	In homozigous form pollen is not viable	(Alonso et al., 2003), (Wang et al., 2013)
	clc2	AT2G20760	Numerous developmental defects	
	clc3	AT3G51890	Numerous developmental defects	
AP-2	*ap2m*	AT5G46630	Showed many developmental defects, including abnormal phyllotaxis, an increase in the number of shoots and branches, smaller leaves, an increase in the leaf number, and shorter root hairs	(Alonso et al., 2003), (Bashline et al., 2013, Kim et al., 2013, Yamaoka et al., 2013)
	ap2s	AT1G47830	Localization and dynamics of CLC-EGFP are altered	(Alonso et al., 2003), (Fan et al., 2013)
AP180	*ap180*	AT2G25430	No obvious growth or developmental defects were observed	(Alonso et al., 2003), (Kaneda et al., 2019)
Dynamins	*drp1a*	AT5G42080	Inhibits fertilization due to maternal sporophytic defect	(Alonso et al., 2003), (Kang et al., 2003a)
	drp1c	AT1G14830	Homozygous lethal (disrupts post-meiotic pollen development)	(Kang et al., 2003b)
	drp1e	AT3G60190	Null mutants have defects of cell plate formation in root and arrest of embryo development; enhanced cell death in response to powdery mildew infection	(Alonso et al., 2003), (Fujimoto and Tsutsumi, 2014, Tang et al., 2006),
	drp2a	AT1G10290	No obvious growth or developmental defects were observed	(Alonso et al., 2003), (Backues et al., 2010)
	drp2b	AT1G59610	No obvious growth or developmental defects were observed	
Auxilin	*auxilin-like1*	AT4G12780	Phenotypically normal	(Adamowski et al., 2018)
	auxilin-like2	AT4G12770	Phenotypically normal	
TPLATE complex	*tplate*	AT1G07670	Embryo-lethal	(Alonso et al., 2003), (Gadeyne et al., 2014)
	tml	AT5G57460	Embryo-lethal	

	twd40-2	AT5G24710	Reduced rates of membrane dye uptake	(Alonso et al., 2003), (Bashline et al., 2015)

Table S6 – Published and characterized mutant EAP lines

Supplemental References

ADAMOWSKI, M., NARASIMHAN, M., KANIA, U., GLANC, M., DE JAEGER, G. & FRIML, J. 2018. A Functional Study of AUXILIN-LIKE1 and 2, Two Putative Clathrin Uncoating Factors in Arabidopsis. *Plant Cell*, 30**,** 700-716.

ALONSO, J. M., STEPANOVA, A. N., LEISSE, T. J., KIM, C. J., CHEN, H., SHINN, P., STEVENSON, D. K., ZIMMERMAN, J., BARAJAS, P., CHEUK, R., GADRINAB, C., HELLER, C., JESKE, A., KOESEMA, E., MEYERS, C. C., PARKER, H., PREDNIS, L., ANSARI, Y., CHOY, N., DEEN, H., GERALT, M., HAZARI, N., HOM, E., KARNES, M., MULHOLLAND, C., NDUBAKU, R., SCHMIDT, I., GUZMAN, P., AGUILAR-HENONIN, L., SCHMID, M., WEIGEL, D., CARTER, D. E., MARCHAND, T., RISSEEUW, E., BROGDEN, D., ZEKO, A., CROSBY, W. L., BERRY, C. C. & ECKER, J. R. 2003. Genome-wide insertional mutagenesis of Arabidopsis thaliana. *Science,* 301**,** 653-7.

BACKUES, S. K., KORASICK, D. A., HEESE, A. & BEDNAREK, S. Y. 2010. The Arabidopsis dynamin-related protein2 family is essential for gametophyte development. *Plant Cell*, 22**,** 3218-31.

BANDMANN, V., MULLER, J. D., KOHLER, T. & HOMANN, U. 2012. Uptake of fluorescent nano beads into BY2-cells involves clathrin-dependent and clathrin-independent endocytosis. *FEBS Lett*, 586**,** 3626-32.

BARTH, M. & HOLSTEIN, S. E. 2004. Identification and functional characterization of Arabidopsis AP180, a binding partner of plant alphaC-adaptin. *J Cell Sci,* 117**,** 2051-62.

BASHLINE, L., LI, S., ANDERSON, C. T., LEI, L. & GU, Y. 2013. The endocytosis of cellulose synthase in Arabidopsis is dependent on mu2, a clathrin-mediated endocytosis adaptin. *Plant Physiol*, 163**,** 150-60.

BASHLINE, L., LI, S., ZHU, X. & GU, Y. 2015. The TWD40-2 protein and the AP2 complex cooperate in the clathrin-mediated endocytosis of cellulose synthase to regulate cellulose biosynthesis. *Proc Natl Acad Sci U S A*, 112**,** 12870-5.

DEJONGHE, W., KUENEN, S., MYLLE, E., VASILEVA, M., KEECH, O., VIOTTI, C., SWERTS, J., FENDRYCH, M., ORTIZ-MOREA, F. A., MISHEV, K., DELANG, S., SCHOLL, S., ZARZA, X., HEILMANN, M., KOURELIS, J., KASPROWICZ, J., NGUYEN LE, S. L., DROZDZECKI, A., VAN HOUTTE, I., SZATMARI, A. M., MAJDA, M., BAISA, G., BEDNAREK, S. Y., ROBERT, S., AUDENAERT, D., TESTERINK, C., MUNNIK, T., VAN DAMME, D., HEILMANN, I., SCHUMACHER, K., WINNE, J., FRIML, J., VERSTREKEN, P. & RUSSINOVA, E. 2016. Mitochondrial uncouplers inhibit clathrin-mediated endocytosis largely through cytoplasmic acidification. *Nat Commun*, 7**,** 11710.

DEJONGHE, W., SHARMA, I., DENOO, B., DE MUNCK, S., LU, Q., MISHEV, K., BULUT, H., MYLLE, E., DE RYCKE, R., VASILEVA, M., SAVATIN, D. V., NERINCKX, W., STAES, A., DROZDZECKI, A., AUDENAERT, D., YPERMAN, K., MADDER, A., FRIML, J., VAN DAMME, D., GEVAERT, K., HAUCKE, V., SAVVIDES, S. N., WINNE, J. & RUSSINOVA, E. 2019. Disruption of endocytosis through chemical inhibition of clathrin heavy chain function. *Nat Chem Biol*, 15**,** 641-649.

DHONUKSHE, P., ANIENTO, F., HWANG, I., ROBINSON, D. G., MRAVEC, J., STIERHOF, Y. D. & FRIML, J. 2007. Clathrin-mediated constitutive endocytosis of PIN auxin efflux carriers in Arabidopsis. *Curr Biol*, 17**,** 520-7.

DI RUBBO, S., IRANI, N. G., KIM, S. Y., XU, Z. Y., GADEYNE, A., DEJONGHE, W., VANHOUTTE, I., PERSIAU, G., EECKHOUT, D., SIMON, S., SONG, K., KLEINE-

VEHN, J., FRIML, J., DE JAEGER, G., VAN DAMME, D., HWANG, I. & RUSSINOVA, E. 2013. The clathrin adaptor complex AP-2 mediates endocytosis of brassinosteroid insensitive1 in Arabidopsis. *Plant Cell,* 25**,** 2986-97.

DUTTA, D., WILLIAMSON, C. D., COLE, N. B. & DONALDSON, J. G. 2012. Pitstop 2 is a potent inhibitor of clathrin-independent endocytosis. *PLoS One,* 7**,** e45799.

ELKIN, S. R., OSWALD, N. W., REED, D. K., METTLEN, M., MACMILLAN, J. B. & SCHMID, S. L. 2016. Ikarugamycin: A Natural Product Inhibitor of Clathrin-Mediated Endocytosis. *Traffic,* 17**,** 1139-49.

FAN, L., HAO, H., XUE, Y., ZHANG, L., SONG, K., DING, Z., BOTELLA, M. A., WANG, H. & LIN, J. 2013. Dynamic analysis of Arabidopsis AP2 sigma subunit reveals a key role in clathrin-mediated endocytosis and plant development. *Development,* 140**,** 3826-37.

FUJIMOTO, M., ARIMURA, S., NAKAZONO, M. & TSUTSUMI, N. 2008. Arabidopsis dynamin-related protein DRP2B is co-localized with DRP1A on the leading edge of the forming cell plate. *Plant Cell Rep,* 27**,** 1581-6.

FUJIMOTO, M. & TSUTSUMI, N. 2014. Dynamin-related proteins in plant post-Golgi traffic. *Front Plant Sci,* 5**,** 408.

GADEYNE, A., SANCHEZ-RODRIGUEZ, C., VANNESTE, S., DI RUBBO, S., ZAUBER, H., VANNESTE, K., VAN LEENE, J., DE WINNE, N., EECKHOUT, D., PERSIAU, G., VAN DE SLIJKE, E., CANNOOT, B., VERCRUYSSE, L., MAYERS, J. R., ADAMOWSKI, M., KANIA, U., EHRLICH, M., SCHWEIGHOFER, A., KETELAAR, T., MAERE, S., BEDNAREK, S. Y., FRIML, J., GEVAERT, K., WITTERS, E., RUSSINOVA, E., PERSSON, S., DE JAEGER, G. & VAN DAMME, D. 2014. The TPLATE adaptor complex drives clathrin-mediated endocytosis in plants. *Cell,* 156**,** 691-704.

HUANG, J., FUJIMOTO, M., FUJIWARA, M., FUKAO, Y., ARIMURA, S. & TSUTSUMI, N. 2015. Arabidopsis dynamin-related proteins, DRP2A and DRP2B, function coordinately in post-Golgi trafficking. *Biochem Biophys Res Commun,* 456**,** 238-44.

HUNTER, K., KIMURA, S., ROKKA, A., TRAN, H. C., TOYOTA, M., KUKKONEN, J. P. & WRZACZEK, M. 2019. CRK2 Enhances Salt Tolerance by Regulating Callose Deposition in Connection with PLDalpha1. *Plant Physiol,* 180**,** 2004-2021.

KANEDA, M., VAN OOSTENDE-TRIPLET, C., CHEBLI, Y., TESTERINK, C., BEDNAREK, S. Y. & GEITMANN, A. 2019. Plant AP180 N-Terminal Homolog Proteins Are Involved in Clathrin-Dependent Endocytosis during Pollen Tube Growth in Arabidopsis thaliana. *Plant Cell Physiol,* 60**,** 1316-1330.

KANG, B. H., BUSSE, J. S. & BEDNAREK, S. Y. 2003a. Members of the Arabidopsis dynamin-like gene family, ADL1, are essential for plant cytokinesis and polarized cell growth. *Plant Cell,* 15**,** 899-913.

KANG, B. H., RANCOUR, D. M. & BEDNAREK, S. Y. 2003b. The dynamin-like protein ADL1C is essential for plasma membrane maintenance during pollen maturation. *Plant J,* 35**,** 1-15.

KIM, S. Y., XU, Z. Y., SONG, K., KIM, D. H., KANG, H., REICHARDT, I., SOHN, E. J., FRIML, J., JUERGENS, G. & HWANG, I. 2013. Adaptor protein complex 2-mediated endocytosis is crucial for male reproductive organ development in Arabidopsis. *Plant Cell,* 25**,** 2970-85.

KITAKURA, S., VANNESTE, S., ROBERT, S., LOFKE, C., TEICHMANN, T., TANAKA, H. & FRIML, J. 2011. Clathrin mediates endocytosis and polar distribution of PIN auxin transporters in Arabidopsis. *Plant Cell,* 23**,** 1920-31.

KONOPKA, C. A., BACKUES, S. K. & BEDNAREK, S. Y. 2008. Dynamics of Arabidopsis dynamin-related protein 1C and a clathrin light chain at the plasma membrane. *Plant Cell,* 20**,** 1363-80.

KONOPKA, C. A. & BEDNAREK, S. Y. 2008. Comparison of the dynamics and functional redundancy of the Arabidopsis dynamin-related isoforms DRP1A and DRP1C during plant development. *Plant Physiol,* 147**,** 1590-602.

LARSON, E. R., VAN ZELM, E., ROUX, C., MARION-POLL, A. & BLATT, M. R. 2017. Clathrin Heavy Chain Subunits Coordinate Endo- and Exocytic Traffic and Affect Stomatal Movement. *Plant Physiol,* 175**,** 708-720.

MOSCATELLI, A., CIAMPOLINI, F., RODIGHIERO, S., ONELLI, E., CRESTI, M., SANTO, N. & IDILLI, A. 2007. Distinct endocytic pathways identified in tobacco pollen tubes using charged nanogold. *J Cell Sci,* 120**,** 3804-19.

MRAVEC, J., PETRASEK, J., LI, N., BOEREN, S., KARLOVA, R., KITAKURA, S., PAREZOVA, M., NARAMOTO, S., NODZYNSKI, T., DHONUKSHE, P., BEDNAREK, S. Y., ZAZIMALOVA, E., DE VRIES, S. & FRIML, J. 2011. Cell plate restricted association of DRP1A and PIN proteins is required for cell polarity establishment in Arabidopsis. *Curr Biol,* 21**,** 1055-60.

ORTIZ-MOREA, F. A., SAVATIN, D. V., DEJONGHE, W., KUMAR, R., LUO, Y., ADAMOWSKI, M., VAN DEN BEGIN, J., DRESSANO, K., PEREIRA DE OLIVEIRA, G., ZHAO, X., LU, Q., MADDER, A., FRIML, J., SCHERER DE MOURA, D. & RUSSINOVA, E. 2016. Danger-associated peptide signaling in Arabidopsis requires clathrin. *Proc Natl Acad Sci U S A,* 113**,** 11028-33.

OWEN, D. J. & EVANS, P. R. 1998. A structural explanation for the recognition of tyrosine-based endocytotic signals. *Science,* 282**,** 1327-32.

ROBERT, S., KLEINE-VEHN, J., BARBEZ, E., SAUER, M., PACIOREK, T., BASTER, P., VANNESTE, S., ZHANG, J., SIMON, S., COVANOVA, M., HAYASHI, K., DHONUKSHE, P., YANG, Z., BEDNAREK, S. Y., JONES, A. M., LUSCHNIG, C., ANIENTO, F., ZAZIMALOVA, E. & FRIML, J. 2010. ABP1 mediates auxin inhibition of clathrin-dependent endocytosis in Arabidopsis. *Cell,* 143**,** 111-21.

SHARFMAN, M., BAR, M., EHRLICH, M., SCHUSTER, S., MELECH-BONFIL, S., EZER, R., SESSA, G. & AVNI, A. 2011. Endosomal signaling of the tomato leucine-rich repeat receptor-like protein LeEix2. *Plant J,* 68**,** 413-23.

TAHARA, H., YOKOTA, E., IGARASHI, H., ORII, H., YAO, M., SONOBE, S., HASHIMOTO, T., HUSSEY, P. J. & SHIMMEN, T. 2007. Clathrin is involved in organization of mitotic spindle and phragmoplast as well as in endocytosis in tobacco cell cultures. *Protoplasma,* 230**,** 1-11.

TANG, D., ADE, J., FRYE, C. A. & INNES, R. W. 2006. A mutation in the GTP hydrolysis site of Arabidopsis dynamin-related protein 1E confers enhanced cell death in response to powdery mildew infection. *Plant J,* 47**,** 75-84.

TAYLOR, M. J., PERRAIS, D. & MERRIFIELD, C. J. 2011. A high precision survey of the molecular dynamics of mammalian clathrin-mediated endocytosis. *PLoS Biol,* 9**,** e1000604.

VAN DAMME, D., GADEYNE, A., VANSTRAELEN, M., INZE, D., VAN MONTAGU, M. C., DE JAEGER, G., RUSSINOVA, E. & GEELEN, D. 2011. Adaptin-like protein TPLATE and clathrin recruitment during plant somatic cytokinesis occurs via two distinct pathways. *Proc Natl Acad Sci U S A,* 108**,** 615-20.

VON KLEIST, L., STAHLSCHMIDT, W., BULUT, H., GROMOVA, K., PUCHKOV, D., ROBERTSON, M. J., MACGREGOR, K. A., TOMILIN, N., PECHSTEIN, A., CHAU, N., CHIRCOP, M., SAKOFF, J., VON KRIES, J. P., SAENGER, W., KRAUSSLICH, H. G., SHUPLIAKOV, O., ROBINSON, P. J., MCCLUSKEY, A. & HAUCKE, V.

2011. Role of the clathrin terminal domain in regulating coated pit dynamics revealed by small molecule inhibition. *Cell,* 146**,** 471-84.

WANG, C., YAN, X., CHEN, Q., JIANG, N., FU, W., MA, B., LIU, J., LI, C., BEDNAREK, S. Y. & PAN, J. 2013. Clathrin light chains regulate clathrin-mediated trafficking, auxin signaling, and development in Arabidopsis. *Plant Cell,* 25**,** 499-516.

YAMAOKA, S., SHIMONO, Y., SHIRAKAWA, M., FUKAO, Y., KAWASE, T., HATSUGAI, N., TAMURA, K., SHIMADA, T. & HARA-NISHIMURA, I. 2013. Identification and dynamics of Arabidopsis adaptor protein-2 complex and its involvement in floral organ development. *Plant Cell,* 25**,** 2958-69.

YOSHINARI, A., FUJIMOTO, M., UEDA, T., INADA, N., NAITO, S. & TAKANO, J. 2016. DRP1-Dependent Endocytosis is Essential for Polar Localization and Boron-Induced Degradation of the Borate Transporter BOR1 in Arabidopsis thaliana. *Plant Cell Physiol,* 57**,** 1985-2000.

ZHANG, H. M., COLYVAS, K., PATRICK, J. W. & OFFLER, C. E. 2017. A Ca2+-dependent remodelled actin network directs vesicle trafficking to build wall ingrowth papillae in transfer cells. *J Exp Bot,* 68**,** 4749-4764.